

Metabolic strategies of free-living and aggregate-associated bacterial communities inferred from biologic and chemical profiles in the Black Sea suboxic zone

Clara A. Fuchsman¹, John B. Kirkpatrick¹, William J. Brazelton¹, James W. Murray¹
& James T. Staley²

¹School of Oceanography, University of Washington, Seattle, WA, USA; and ²Department of Microbiology, University of Washington, Seattle, WA, USA

Correspondence: Clara A. Fuchsman, School of Oceanography, University of Washington, Box 355351, Seattle, WA 98195-5351, USA. Tel.: +1 206 543 9669; fax: +1 206 685 3351; e-mail: cfuchs1@u.washington.edu

Received 4 August 2010; revised 8 July 2011; accepted 14 August 2011.

Final version published online 19 September 2011.

DOI: 10.1111/j.1574-6941.2011.01189.x

Editor: Patricia Sobczyk

Keywords

manganese oxidation; nitrate reduction; microaerophilic; methane oxidation; particle attached.

Abstract

The Black Sea is a permanently anoxic basin with a well-defined redox gradient. We combine environmental 16S rRNA gene data from clone libraries, terminal restriction fragment length polymorphisms, and V6 hypervariable region pyrosequences to provide the most detailed bacterial survey to date. Furthermore, this data set is informed by comprehensive geochemical data; using this combination of information, we put forward testable hypotheses regarding possible metabolisms of uncultured bacteria from the Black Sea's suboxic zone (microaerophily, nitrate reduction, manganese cycling, and oxidation of methane, ammonium, and sulfide). Dominant bacteria in the upper suboxic zone included members of the SAR11, SAR324, and *Microthrix* groups and in the deep suboxic zone included members of BS-GSO-2, Marine Group A, and SUP05. A particulate fraction (30 µm filter) was used to distinguish between free-living and aggregate-associated communities in the suboxic zone. The particulate fraction contained greater diversity of V6 tag sequences than the bulk water samples. *Lentisphaera*, *Epsilonproteobacteria*, WS3, *Planctomycetes*, and *Deltaproteobacteria* were enriched in the particulate fraction, whereas SAR11 relatives dominated the free-living fraction. On the basis of the bacterial assemblages and simple modeling, we find that in suboxic waters, the interior of sinking aggregates potentially support manganese reduction, sulfate reduction, and sulfur oxidation.

Introduction

The Black Sea, a semi-enclosed basin, contains at least three distinct microbial ecosystems. The surface layer of the Black Sea is well-oxygenated and driven by oxygenic photosynthetic processes, whereas the aphotic deep layer is anoxic and sulfidic. A suboxic zone (c. 50 m thick) lies at the boundary between the oxic and anoxic layers. The suboxic zone, which has < 10 µM oxygen and undetectable hydrogen sulfide (Murray *et al.*, 1995) hosts a variety of microbial metabolisms including anoxygenic photosynthesis, manganese oxidation, nitrification, denitrification, and anammox (Kuypers *et al.*, 2003; Manske *et al.*, 2005; Lam *et al.*, 2007; Oakley *et al.*, 2007; Clement *et al.*,

2009). The hydrological balance is influenced by freshwater input from rivers such as the Danube, which mix into surface waters, whereas salty Mediterranean waters flow through the Bosphorus Strait and fill the deep basin. These two different water sources cause the Black Sea to be permanently stratified with respect to salinity and density, and this has led to physical, chemical (Caspers, 1957; Sorokin, 1983), and therefore microbial stratification of the Black Sea's water column.

The Black Sea is an ideal place to study microbially mediated redox reactions in low oxygen conditions. The vertical scale of the highly stable redox gradient is in the order of meters to tens of meters, providing the opportunity to finely sample the sequence of redox reactions

(Murray *et al.*, 1995). Nonetheless, bacterial communities of the Black Sea suboxic zone have not been thoroughly studied. Other researchers have examined bacterial functional genes (Lam *et al.*, 2007; Oakley *et al.*, 2007), specific bacterial groups in the suboxic layer (Manske *et al.*, 2005; Kirkpatrick *et al.*, 2006; Schubert *et al.*, 2006), or bacteria in the sulfidic zone (e.g. Grote *et al.*, 2008; Glaubitz *et al.*, 2010). Lin *et al.* (2006) quantified some phylum-level groups in the suboxic zone using FISH, but only Vetriani *et al.* (2003) examined species-level diversity of the general bacterial community.

Due to the stratification of the Black Sea, characteristic inflections in the water-column profiles of nitrate, manganese, cesium isotopes, and mesoplankton, etc. are associated with specific density values, but not with specific depths, regardless of when and where they were sampled (Vinogradov & Nalbandov, 1990; Buesseler *et al.*, 1991; Codispoti *et al.*, 1991; Lewis & Landing, 1991; Murray *et al.*, 1995). Therefore, results presented here will be plotted against potential density (σ_θ) rather than depth (m). Both axes are used in Fig. 1 for comparison.

In most of the Black Sea, the oxygenated cold intermediate layer (core density of $\sigma_\theta = 14.5$) represents the lower boundary of direct communication with the surface; the ventilation frequency of this layer depends on winter conditions (Tolmazin, 1985; Gregg & Yakushev, 2005). However, the suboxic layer is still linked to euphotic processes via the sinking of organic matter. In marine systems, organic matter aggregates have been found to be enriched in nutrients and to exhibit higher bacterial abundance and enzyme activity compared with the water

column (Simon *et al.*, 2002). The bacterial communities of free-living and aggregate-attached bacteria have been reported to be taxonomically distinct in marine environments (e.g. DeLong *et al.*, 1993; Kellogg & Deming, 2009), but aggregate-attached bacterial communities in suboxic waters have not been previously examined.

In this article, we report the most comprehensive census of microbial diversity for the suboxic Black Sea published to date, and we examine the contribution of sinking aggregates to the taxonomic composition of the suboxic zone. Many bacteria in the Black Sea are not closely related to cultured organisms (Vetriani *et al.*, 2003) and have unknown metabolisms. Therefore, in addition to describing our census of diversity, we attempt to make testable hypotheses regarding the likely metabolisms of uncultured organisms by linking our biological data to a comprehensive suite of chemical measurements. Our biological data includes three complementary and independent datasets: full-length 16S rRNA gene clone libraries, V6 hypervariable region tag pyrosequences, and terminal restriction fragment length polymorphism (TRFLP) profiles. The large number of V6 tags (*c.* 9000 per sample) allows deep examination of diversity and community similarities, whereas TRFLP analyses of many samples yield a detailed depth profile. Our integration of multiple biologic and chemical datasets represents the most thorough description of Black Sea microbial ecology to date.

Materials and methods

Sampling

DNA samples were collected in the western central gyre of the Black Sea in late March 2005 on cruise 403 of the *R/V Endeavor* (42°30' N, 30°45' E). Samples were collected using a CTD-Rosette with 10-L Niskin bottles and Sea Bird sensors. Approximately 2 L of sample were filtered into 0.2- μ m Millipore Sterivex filters for bulk water. Aggregate-associated samples were collected using a 30- μ m flat polypropylene filter (Millipore) from a separate cast at the same station. Samples were immediately frozen and stored at -80 °C upon arrival in the laboratory. Some full-length sequences were also obtained from samples collected in the same manner in April 2003 on Voyage 162 leg 17 of the *R/V Knorr* (42°30' N, 31°00' E).

DNA extraction

The DNA extraction protocol was adapted from Vetriani *et al.* (2003) and included 8–10 freeze thaw cycles between a dry ice/ethanol bath and a 55 °C water bath followed by chemical lysis with lysozyme and proteinase

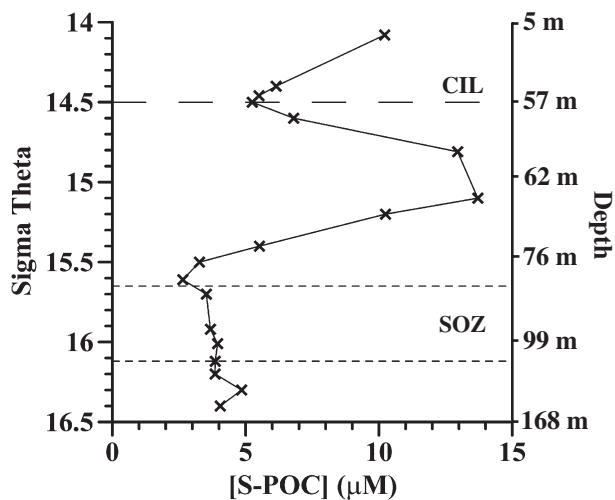


Fig. 1. Concentration of suspended particulate organic carbon. Both potential density and depth axes are shown for comparison. Dotted lines indicate the borders of the suboxic zone. Dashed line indicates the cold intermediate layer (CIL).

K. All DNA used for V6 tag amplification and TRFLP was extracted in this fashion. The 30 μm filter used for 16S rRNA gene clone libraries was extracted with an additional bead beating step utilizing 0.1 and 0.5 mm zirconia-silica beads.

Amplification of 16S rRNA gene V6 hypervariable region

Four samples from March 2005 were amplified targeting the V6 hypervariable region of 16S rRNA gene: bulk water from densities $\sigma_\theta = 15.34, 15.79, 16.08$, and a 30 μm filter from $\sigma_\theta = 15.8$. V6 amplicon libraries were constructed and sequenced as in Huber *et al.* (2007). PCR amplification, in 30 cycles, used 0.2 μM of each primer in a cocktail of five forward primers (967F) and four reverse primers (1046R; as per Huber *et al.*, 2007). Multiple primers were used to increase taxonomic coverage. Eighty-nine percent of all sequences in the Greengenes database (DeSantis *et al.*, 2006; accessed April 2009) matched the V6 primer set, although 18% of *Planctomyces* sequences had a mismatch.

PCR products were pyrosequenced on a Roche Genome Sequencer FLX in the Sogin lab (Marine Biological Laboratory, Woods Hole, MA) as part of the International Census of Marine Microbes (ICoMM). The resulting tag sequences were screened for quality as recommended by Huse *et al.* (2007). Tag sequences have been deposited in the National Center for Biotechnology Information (NCBI) Short Read Archive (SRA) under the accession numbers SRS005799–SRS005802.

Although we could not obtain replicate pyrosequencing samples, Brazelton *et al.* (2010) obtained two replicate pyrosequencing runs from the same facility. These replicate sequencing runs were performed months apart with different amplicon libraries. The Bray–Curtis similarity of these replicates was 89%, greater than any of the similarity values reported in this study.

Alignment of V6 tags

Bacterial sequence alignments were constructed by submitting the unique V6 tag sequences from all four samples to the *NAST* aligner (<http://greengenes.lbl.gov>). Primers were included to ensure full-length alignment. The alignment was manually corrected and primers were trimmed. The distance matrix for each alignment was calculated with *quickdist* as described in Sogin *et al.* (2006) without penalties for terminal gaps. Sequences were clustered into operational taxonomic units (OTUs), and rarefaction curves and diversity estimators were calculated with *DOTUR* (Schloss & Handelsman, 2005).

Comparisons of V6 tags between samples

The program *SONS* (Schloss & Handelsman, 2006) was used to determine the relative abundance distribution of each OTU in each sample. To normalize the abundances of each sequence type among samples, tags were randomly resampled using *DaisyChopper* (available at <http://www.genomics.ceh.ac.uk/GeneSwytch/Tools.html>). These normalized OTUs were used in Venn diagrams, depth profiles, and Bray–Curtis and Jaccard similarity calculations (calculated with *PRIMER 6* (<http://www.primer-e.com>) without any further data transformation). Bray–Curtis similarities will be shown here as the index utilizes abundance data. Jaccard similarities (presence/absence) are lower, but follow the same trend.

16S rRNA gene clones

Nearly full-length 16S rRNA gene clones were amplified from suboxic water collected from the western central gyre in April 2003, and from $\sigma_\theta = 15.3$ and the 30- μm filter from $\sigma_\theta = 15.8$ in the western central gyre in March 2005. PCR was performed using universal bacterial primers 27F (5'-AGAGTTTGATCCTGGCTCAG-3') and 1492R (5'-GGTTACCTTGTTACGACTT-3') for 32 cycles with annealing at 60 °C (Lane, 1991). Sequencing was done at High-Throughput Sequencing Solutions (<http://www.htseq.org>) using primers T7, M13R, and 357F (Muyzer *et al.*, 1993). Chromatograms were hand-inspected and contigs assembled using the *Sequencher* program (GeneCodes Corporation, Ann Arbor, MI). SSU rRNA gene sequences were deposited at Genbank under the accession numbers GU145386–GU145550.

Taxonomy

Taxonomy was assigned to each V6 tag sequence by the *GAST* process (Huse *et al.*, 2008). Tags with distances > 0.25 were added to the unclassified category. V6 tags were also compared with Black Sea full-length 16S rRNA gene sequences. The V6 regions of the full-length sequences were compared with the V6 tags using *MATGAT 2.0* (Capanella *et al.*, 2003) to obtain distances. The taxonomy of nearly full-length Black Sea sequences was determined by the Greengenes classifier using Hugenholtz taxonomy (<http://greengenes.lbl.gov>). Boot-strapped neighbor-joining trees were created in *Arb* after alignment to a master database using the *NAST* tool of greengenes.lbl.gov. To clarify differences between Marine Group A and *Deferribacteres*, a tree was originally created using sequences used to define the *Deferribacteres* and Marine Group A phyla in Jumas-Bilak *et al.* (2009). To save room, many *Deferribacteres* sequences were removed in the final figure.

TRFLP

TRFLPs were obtained from a profile (14 depths) of the western central gyre in March 2005 using universal bacterial primers 27F-FAM and 1517R (5'-ACGGCTACC TTGTTACGACTT-3') (Vetriani *et al.*, 2003). PCR products were amplified for 30 cycles at 48 °C using 2 × PCR MasterMix (Fermentas, Ontario, Canada). Purified PCR products (QiaQuick columns; Qiagen, Valencia, CA) were separately digested overnight with four restriction enzymes (HaeIII, Hpy188I, MspI, MnlI) and immediately ethanol precipitated according to the manufacturer's instructions (Amersham Pharmacia Dynamics). Analysis was performed on a MegaBACE 1000 apparatus (Molecular Dynamics) at the University of Washington Marine Molecular Biotechnology Laboratory. Electrophoretic profiles were visualized using Dax software (Van Mierlo Software Consultancy, The Netherlands). TRFLP profiles were normalized by total peak height. TRFLP peaks were binned using frame shifting (Hewson & Fuhrman, 2006) with four frames at 0.5-bp intervals. For each enzyme, a resemblance matrix was obtained using either the Bray-Curtis index, which takes abundance (peak height) into account, or the Jaccard index which uses presence/absence, and for each comparison between two samples, the maximum similarity of the four frames was used. Profiles were clustered using the PRIMER 6 program. Error in the resemblance matrix and significance level of the cluster diagram was determined with a Monte-Carlo simulation of 50 replicates using the average standard deviation in both peak height and base pairs as determined by 16 pairs of replicate TRFLP profiles.

Select 16S rRNA gene clone PCR products from 2003 and 2005 were digested with all four restriction enzymes and used to identify TRFLP peaks with a range ± 0.5 bp from the length of the digested clone. For a peak to be considered positively identified as a clone library sequence via TRFLP, corresponding peaks must have been present in electrophoretic profiles produced by two or more endonucleases, and a match must have been made for the shape of peak height profile vs. depth for two or more enzymes.

Due to the replicability of the relative peak heights and the lack of cloning bias (Rainey *et al.*, 1994), and because each PCR was run under the same conditions with similar extracts from the same amount of material, each normalized TRFLP peak was compared between different TRFLP profiles. However, due to PCR bias (Polz & Cavanaugh, 1998), comparison between the heights of different peaks was made with caution. More than one bacterial species can produce the same TRFLP peak; however, by ensuring that the shape of a peak's depth profile must match between more than one enzyme, and using a small bin size, that risk was reduced.

Cell counts

Ten milliliters of water from density surfaces $\sigma_\theta = 15.5$, 15.7, 15.9, and 16.0 was filtered onto a 0.2 μm filter (Millipore) and frozen. DAPI staining was performed in the laboratory, and a minimum of 200 cells were counted.

Chemical data

Oxygen was measured using the classic Winkler method, and sulfide was measured by iodometric titration (Cline, 1969). In both cases, reagents were bubbled with argon to avoid contamination by atmospheric oxygen. Nutrients were analyzed using a two channel Technicon Autoanalyzer II system. Nitrate was reduced to nitrite using a cadmium column, which was measured using sulfanilamide and *N*(1-naphthyl)-ethylenediamine (Armstrong *et al.*, 1967). Ammonium was analyzed using the indophenole blue procedure (Slawky & MacIsaac, 1972). Deep water samples were diluted with nitrate-free Black Sea surface water to reduce sulfide content. Particulate manganese was filtered onto 0.4 μm filters. Oxidized particulate manganese was determined by B. Tebo by reducing the particulate Mn in 0.1% hydroxylamine and then measuring Mn(II) using the formaldoxime method (Brewer & Spencer, 1971) as seen in Konovalov *et al.* (2003).

Methane was measured in water samples collected for N_2/Ar in evacuated 250-mL glass flasks. In the half-full flasks, the water was equilibrated with the headspace overnight and then removed. Gas samples were cryogenically processed and measured at the Stable Isotope Lab, School of Oceanography, University of Washington, on a Finnegan Delta XL isotope ratio mass spectrometer using interfering masses for mass 32 and 16. Millivolts from mass 32 multiplied by the ratio of 16/32 measured for air was subtracted from millivolts of mass 16. The remainder was considered to be mV of methane. Methane data obtained from the sulfidic layer of the Western Central Gyre in 2003 using gas chromatograph methods (A.V. Egorov, unpublished data) was used to calibrate mV of methane ($R^2 = 0.99$) with the assumption that methane concentration at the same density in the sulfidic zone are relatively constant over time, which is consistent with the data of Kessler *et al.* (2006).

V6 tag sequence depth profiles

V6 tag sequences were categorized into five different depth profiles based on the normalized number of tags at each depth using a Perl script. In each category, at least one depth must have had 10 or more tags of that particular sequence, to be sure that enough information existed to categorize the profile properly. Due to the random

nature of the normalization, some OTUs with a low frequency of tags (e.g. Chlorobi phylotype BS130 with 43 original but < 10 normalized tags at $\sigma_\theta = 16.1$) were not categorized, but might become categorized if the normalization were repeated. The five potential metabolic group profile categories (Metabolic Groups I–V) were defined by the following equations. The number of tags of a particular sequence at the density indicated inside the brackets, for example {15.3}, equals the number of tags of a particular sequence at the density $\sigma_\theta = 15.3$.

Metabolic Group I (aerobic; Fig. 6a): $\{15.3\} \geq 10 \text{ tags} \cap 1.55 \times \{15.8\} < \{15.3\} \cap \{16.1\} < 10 \text{ tags}$.

Metabolic Group II (nitrate reduction; Fig. 6b): $\{15.3\} \geq 10 \text{ tags} \cap 1.55 \times \{15.3\} > \{15.8\} > 0.45 \times \{15.3\} \cap \{16.1\}$ is either $< 10 \text{ tags} \cup < 0.03 \times \{15.3\}$.

Metabolic Group III (manganese oxidation; Fig. 6c): $\{15.8\} > 1.55 \times \{15.3\}$ and $> 1.55 \times \{16.1\} \cap \{15.8\} \geq 10 \text{ tags}$.

Metabolic Group IV (methane oxidation or manganese oxide reduction; Fig. 6d): $\{16.1\} \geq 10 \text{ tags}$ and $\geq \{15.8\} \cap \{15.8\} \geq 5 \text{ tags} \cap \{15.3\} < 5 \text{ tags}$.

Metabolic Group V (sulfur cycling; Fig. 6e): $\{15.3\}$ and $\{15.8\} < 5 \text{ tags} \cap \{16.1\} \geq 10 \text{ tags}$.

Tags not fulfilling the requirements for any of these categories were labeled as uncategorized. ‘Aggregate-attached’ and ‘free-living’ designations were also determined with a Perl script (Fig. 5c).

Aggregate-attached only: $[30 \mu\text{m}] \geq 4 \times [15.8] \cap [30 \mu\text{m}] \geq 10 \text{ tags}$.

Free-living only: $[15.8] \geq 5 \times [30 \mu\text{m}] \cap [15.8] \geq 10 \text{ tags}$.

Aggregate-associated and free-living (i.e. abundant on both filters): $[30 \mu\text{m}] < 4 \times [15.8] \cap [15.8] < 5 \times [30 \mu\text{m}] \cap [30 \mu\text{m}] \geq 10 \text{ tags}$.

Cut-offs for aggregate-attached (4× enriched) and free-living (5× enriched) were determined empirically. The classification of OTUs as free-living, versatile, or aggregate-attached did not depend greatly on the threshold criteria. If free-living bacteria were determined by a threshold of 3× more abundance in the bulk water instead of 4×, then three more OTUs would become designated as free-living. If the threshold for aggregate-attached bacteria were changed to 3× more abundance in the particulate sample, then four OTUs would become aggregate-attached.

Results

Chemical profiles

Chemical concentrations and their fluxes at the depths sampled for V6 pyrosequencing are seen in Table 1. Full depth profiles are shown in Fig. S1. Oxygen decreased

Table 1. Combination of advection and diffusion fluxes in $\mu\text{mol m}^{-2} \text{ day}^{-1}$ and concentration in μM for each depth analyzed for V6 tag sequences

	$\sigma_\theta = 15.3$		$\sigma_\theta = 15.8$		$\sigma_\theta = 16.1$	
	Flux	Conc.	Flux	Conc.	Flux	Conc.
O ₂	13 251	39.5	2141	1.8		b.d.
NO ₃ ⁻	22*	4.8	208	2.1		b.d.
NH ₄ ⁺		b.d.	127	0.006	312	2
CH ₄		b.d.	14	b.d.	34	0.2
H ₂ S		b.d.		b.d.	107	b.d.
PMn	No gradient	0.016	920	0.054	2.8	0.031

b.d., below detection. Fluxes were calculated using mixing coefficients from Ivanov & Samodurov (2001).

*At the nitrate maximum, diffusion was a negative flux.

from 335 μM at the surface ($\sigma_\theta = 14.29$) to 10 μM at $\sigma_\theta = 15.65$, and was undetectable below $\sigma_\theta = 16.0$ ($\sigma_\theta = 17.21$). The first detectable sulfide (3 μM ; Kononov *et al.*, 2003) was at $\sigma_\theta = 16.11$, which was slightly deeper than the deepest V6 sample ($\sigma_\theta = 16.08$). Sulfide then increased to 380 μM in the deep water. Nitrate was below 0.1 μM for the top 58 m of the Black Sea ($\sigma_\theta = 14.47$) but then increased to a maximum of 4.8 μM at $\sigma_\theta = 15.38$ and then decreased to undetectable at $\sigma_\theta = 15.9$. Nitrite had a maximum of 0.09 μM at $\sigma_\theta = 15.85$. Ammonium concentrations were 0.08 μM at $\sigma_\theta = 15.85$ and increased to 2.9 μM at the bottom of the suboxic zone and then to 98 μM at depth. Methane was first measurable at $\sigma_\theta = 15.85$, and then increased to 0.4 μM at the bottom of the suboxic zone and to 13.5 μM at 750 m ($\sigma_\theta = 17.15$). The concentration of particulate manganese was variable, but low in the oxycline. Particulate manganese had a maximum of 0.22 μM at $\sigma_\theta = 15.85$ and decreased to *c.* 0.01 μM in deeper water.

Suspended particulate carbon (S-POC) concentrations are shown in Fig. 1. S-POC was 10.2 μM at 20 m in the euphotic zone, and then decreased to between 5 and 7 μM from 50 to 57 m ($\sigma_\theta = 14.4$ – 14.6). S-POC increased to 13.7 μM at $\sigma_\theta = 15.1$, and then decreased to 4 μM in the suboxic zone.

Microbial data

TRFLP chromatograms were obtained from 14 depths including nine in the hypoxic/suboxic region. These TRFLP chromatograms (MspI) illustrate the bacterial community shifts with depth (Figs S2–S4). Comparison of TRFLP profiles (Fig. S2) indicate that all the low oxygen bacterial communities were significantly different (< 25% similarity) both from the community at higher oxygen concentrations and from the community in the deep sulfidic zone ($\sigma_\theta = 16.8$ [275 m], 17.19 [1000 m])

and 17.21 [2000 m]). However, $\sigma_0 = 16.1$ shared some of the bacterial community (41% similarity) with the sulfidic sample $\sigma_0 = 16.4$ (141 m). Interestingly, samples from the suboxic zone formed three separate bacterial communities within a larger coherent cluster (Fig. S2): upper suboxic ($\sigma_0 = 15.3$ –15.7), lower suboxic ($\sigma_0 = 15.75$ –15.95), and deep suboxic/upper sulfidic ($\sigma_0 = 16.0$ –16.4). The water samples used in pyrosequencing represent these three distinct bacterial communities, and span varying oxygen and nutrient concentrations (Table 1; Fig. S1).

We obtained 36 342 high quality bacterial V6 tag sequences from four samples, representing a total of 2088 OTUs at 0.03 distance (97% similarity) with a range of 726–888 OTUs and 7761–10 566 tags per sample. We identified 18 of the OTUs in TRFLP profiles (30% of TRFLP peaks) by linking V6 tag sequences to corresponding full-length 16S rRNA gene clones. The taxonomic composition of each sample, based on V6 pyrosequences, is

shown in Fig. 2 (first column). The most frequently occurring V6 tag sequences in each sample are shown in the second column of Fig. 2. The most dominant sequence in the $\sigma_0 = 15.3$ and 15.8 samples matched the full-length sequence BS007 from group II of the SAR11 clade of *Alpha-proteobacteria* (Fig. 3), which are typically oligotrophic heterotrophs found in the mesopelagic ocean (Carlson *et al.*, 2009). An uncultured member of the *Gammaproteobacteria*, which matched full-length sequence BS129 from group BS-GSO2 (Fig. 3), was the most dominant V6 sequence at $\sigma_0 = 16.1$. BS129 was quite closely related to I18-19 (GU108534) (Fig. 3), which was found to be autotrophic during stable isotope probing of the upper sulfidic zone of the Black Sea (Glaubitz *et al.*, 2010). The SAR324 group of *Deltaproteobacteria* was abundant in every sample. However, the SAR324 V6 tag sequence abundant at $\sigma_0 = 15.3$ could not be linked to a full-length clone sequence. V6 tags matching BS134 dominated at $\sigma_0 = 15.8$. V6 tags matching

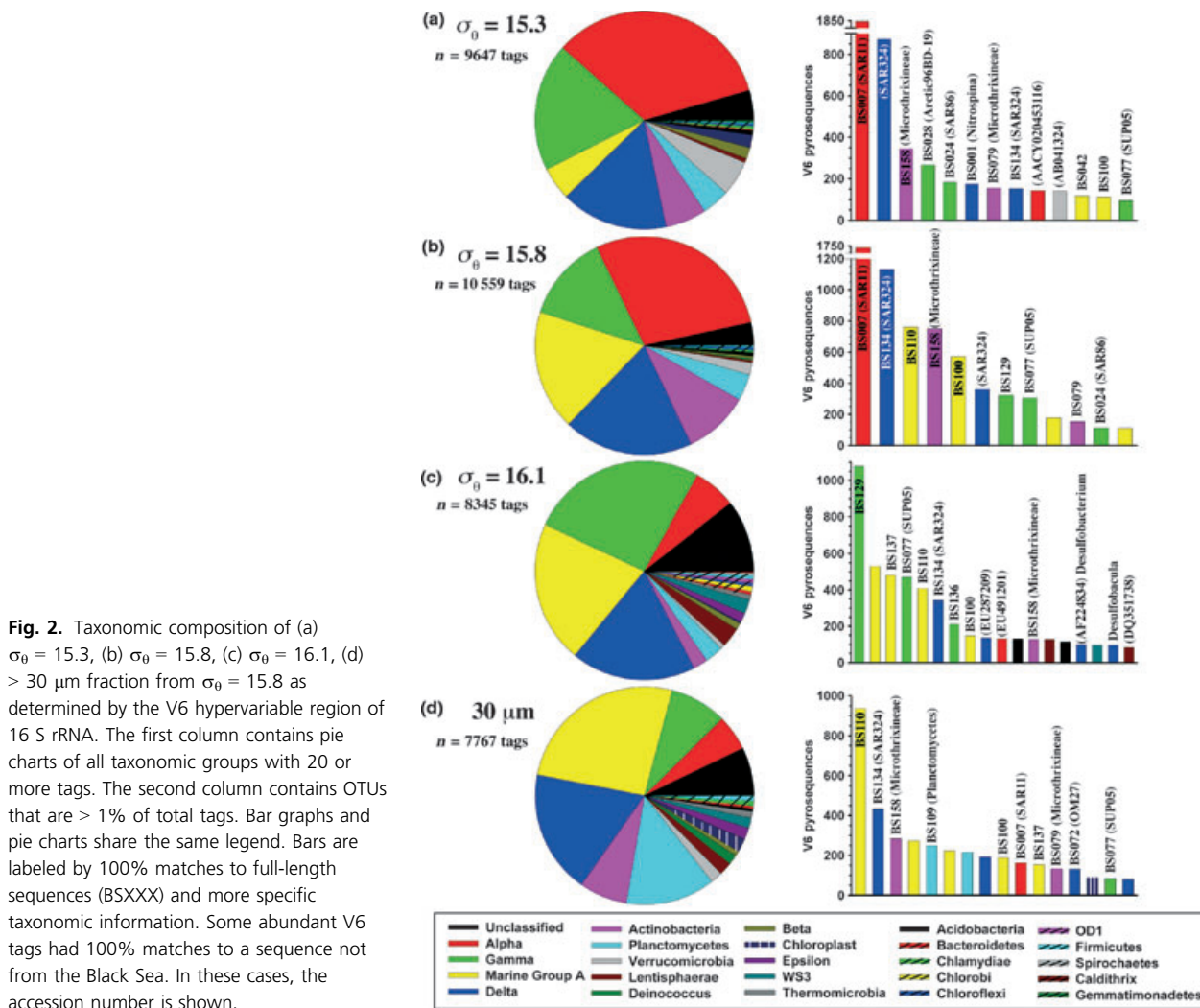


Fig. 2. Taxonomic composition of (a) $\sigma_0 = 15.3$, (b) $\sigma_0 = 15.8$, (c) $\sigma_0 = 16.1$, (d) $> 30 \mu\text{m}$ fraction from $\sigma_0 = 15.8$ as determined by the V6 hypervariable region of 16S rRNA. The first column contains pie charts of all taxonomic groups with 20 or more tags. The second column contains OTUs that are $> 1\%$ of total tags. Bar graphs and pie charts share the same legend. Bars are labeled by 100% matches to full-length sequences (BSXXX) and more specific taxonomic information. Some abundant V6 tags had 100% matches to a sequence not from the Black Sea. In these cases, the accession number is shown.

BS158 and BS079, Actinobacteria related to the deeply branching microaerophilic heterotroph *Microthrix parvicella* (Rossetti et al., 2005; Fig. 4), were also present in all samples. V6 tags matching BS110, a member of Marine Group A (Fig. 4), dominated the aggregate sample along with tags matching BS134 (SAR324), BS158 (*Microthrix*), and BS109, an unclassified *Planctomycetes* (Fig. 4). BS109 primarily groups with other Black Sea sequences sequenced using *Planctomycetes* specific primer sets (Fig. 4; Kirkpatrick et al., 2006; Woebken et al., 2008).

The GAST process, which utilizes SILVA taxonomy (Huse et al., 2008), assigned many tag sequences as *Deferribacteres*. However, all '*Deferribacteres*' sequences from the GAST database with matches to Black Sea tags appear to belong to Marine Group A (Fig. 4). Pyrosequences from this uncultured phylum (BS110, BS100, BS137, BS042) are found in all four samples.

While all V6 tag samples were obtained from depths containing low oxygen and no measurable sulfide, the

39 μM oxygen ($\sigma_0 = 15.3$) (Fig. 2a) and the undetectable oxygen ($\sigma_0 = 16.1$) (Fig. 2c) samples had dissimilar bacterial communities (11% Bray–Curtis similarity), whereas the 39 μM oxygen ($\sigma_0 = 15.3$) and 2 μM oxygen samples ($\sigma_0 = 15.8$) (Fig. 2b) had more similar communities (51% Bray–Curtis). The 30 μM oxygen ($\sigma_0 = 15.3$) and 2 μM oxygen ($\sigma_0 = 15.8$) samples also share more OTUs (248) than do the 2 μM oxygen and the deep suboxic zone samples ($\sigma_0 = 16.1$) (154) (Fig. 5b). The bacterial community on the 30 μm filter was most similar (43%) to the community from bulk water from the same depth ($\sigma_0 = 15.8$), but was more similar to the sample from $\sigma_0 = 16.1$ (33%) than to $\sigma_0 = 15.3$ (24%). The particulate sample shared significant OTUs with all three depths (Fig. 5b), but shared many OTUs (111), otherwise only found at $\sigma_0 = 16.1$.

The diversity between samples varied greatly. The undetectable oxygen sample ($\sigma_0 = 16.1$) and particulate sample ($\sigma_0 = 15.8$) showed significantly more diversity

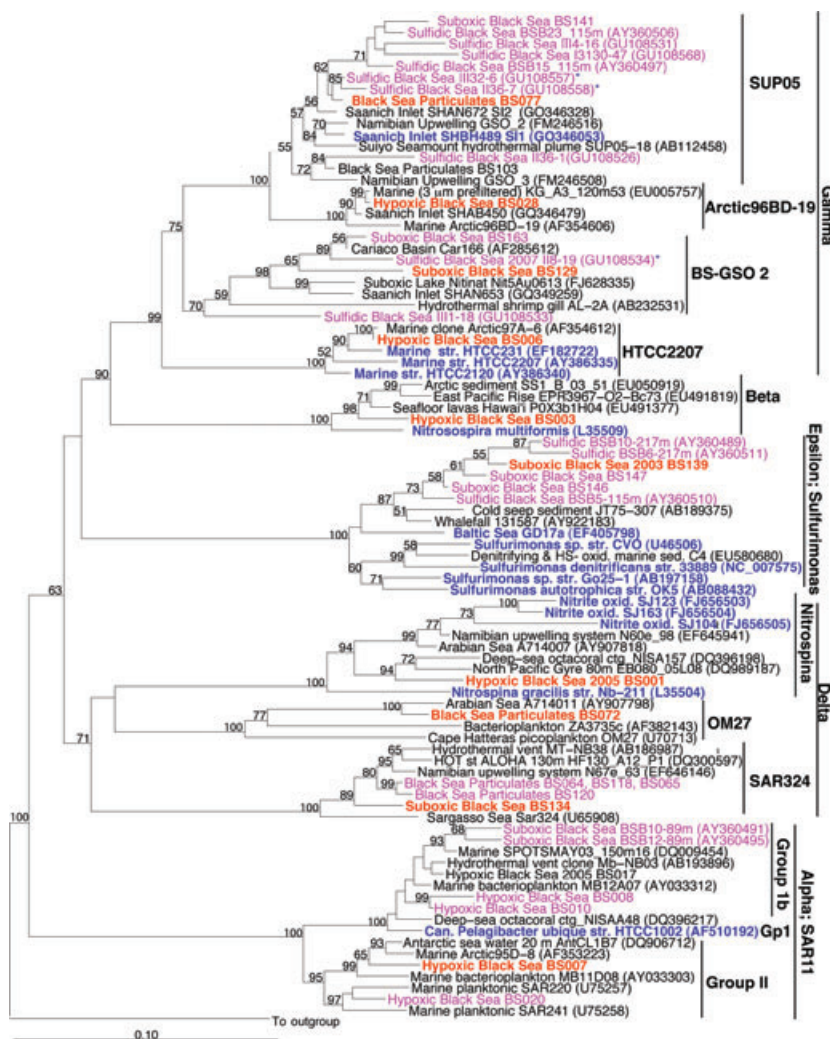


Fig. 3. A neighbor-joining phylogenetic tree of proteobacterial groups important in the Black Sea suboxic zone. Black Sea sequences discussed in the text are in red. Other Black Sea sequences (from this work or from Vetriani et al., 2003 or Glaubitiz et al., 2010) are shown in pink. Cultured, enriched, or sequenced organisms are in blue. Asterisks indicate autotrophic bacteria identified using stable isotope probing with bicarbonate (Glaubitiz et al., 2010). Outgroup is *Flexibacter litoralis* (M58784).

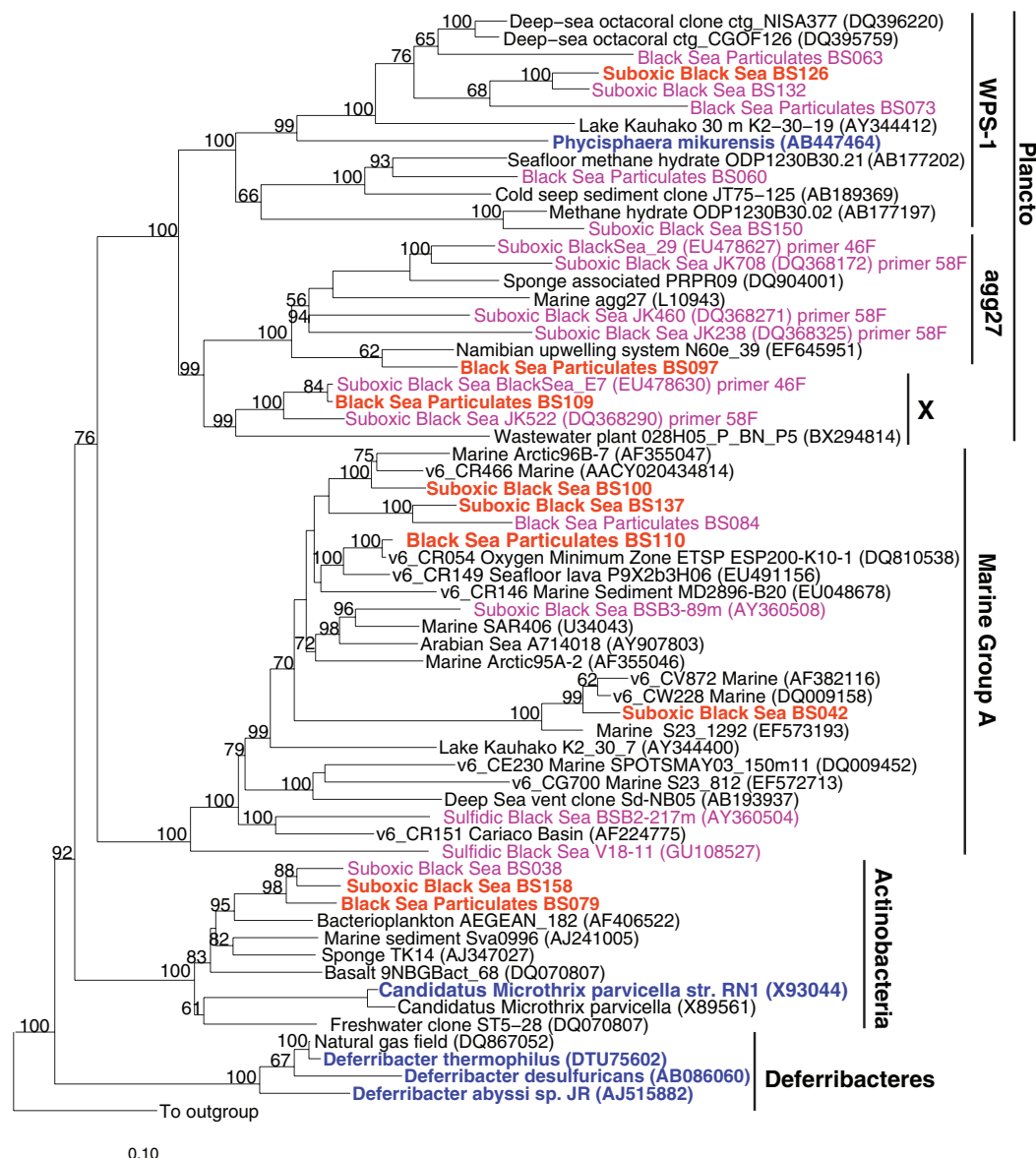


Fig. 4. A neighbor-joining phylogenetic tree of nonproteobacterial groups important in the Black Sea suboxic zone. Black Sea sequences discussed in the text are in red. Other Black Sea sequences (Vetriani *et al.*, 2003; Kirkpatrick *et al.*, 2006; Woebken *et al.*, 2008; Glaubitz *et al.*, 2010) are shown in pink. Cultured, enriched or sequenced organisms are in blue. This tree indicates that Marine Group A, not *Deferribacteres*, is an important phylum in the Black Sea. The tree was created using sequences used to define the Marine Group A phyla in Jumas-Bilak *et al.* (2009). Sequences with names starting with V6 were used in the GAST process (Huse *et al.*, 2008) to assign Black Sea V6 tags. Outgroup is *Thermotoga* sp str KOL6.

than the bulk water samples with low (30 μM ; $\sigma_0 = 15.3$) or very low (2 μM oxygen; $\sigma_0 = 15.8$) oxygen levels, as seen in rarefaction curves (Fig. 5a). Chao1 indices for the samples range from 900 to 1250, indicating significantly less diversity than seen in Atlantic Ocean seawater with similar sequencing effort (Chao1 = 13 772) (Sogin *et al.*, 2006). Even when all Black Sea samples were pooled, they showed less diversity (Chao1 = 3529).

Comparison between methods

Pyrosequencing and TRFLP both avoid cloning biases (Rainey *et al.*, 1994), but still contain PCR biases (Polz & Cavanaugh, 1998; Huse *et al.*, 2007, 2008). Despite the use of different primers, conclusions from TRFLP data and V6 tag sequences compare well. We can identify many of the same OTUs using both techniques. Not only are depth profiles of individual OTUs similar between

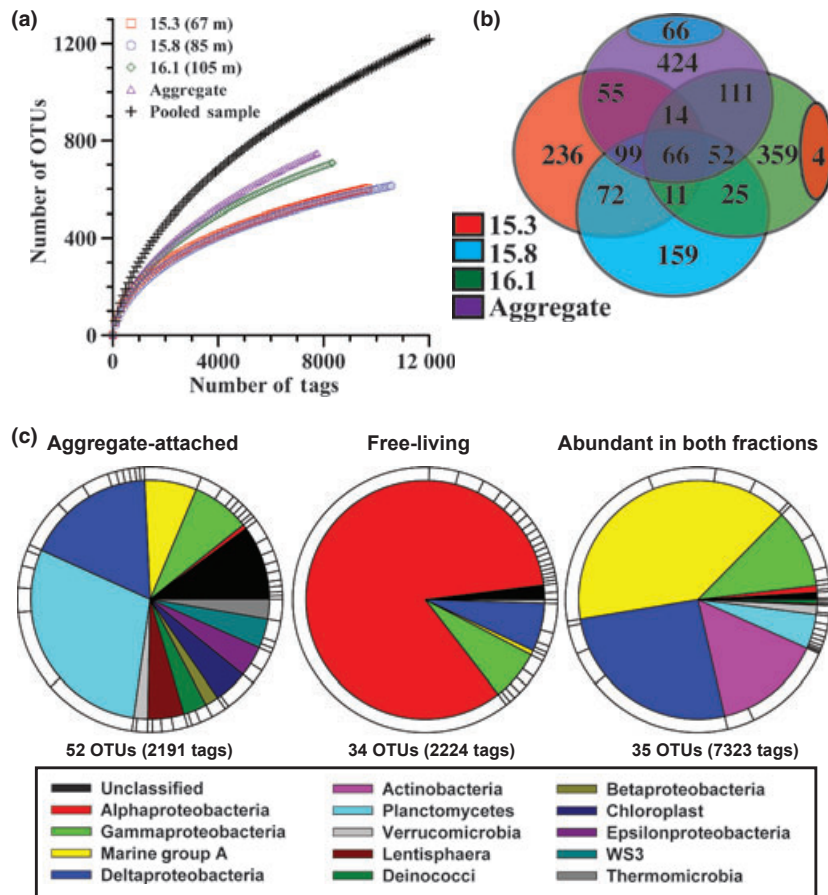


Fig. 5. Comparison of samples from which V6 tag sequences were obtained. (a) Rarefaction curves of OTUs at 0.03 distance for the four samples with V6 tags and a pooled sample combining all four samples. The pooled sample includes 36 342 tags and 2088 OTUs, but the entire curve is not shown for clarity. (b) Venn diagram of OTUs at 0.03 distance shared by the four samples. The small ovals indicate that four OTUs were shared only between $\sigma_0 = 15.3$ and $\sigma_0 = 16.1$, whereas 66 OTUs were shared only between $\sigma_0 = 15.8$ and the aggregate-associated sample. (c) The broad taxonomic designations of aggregate-attached (5 \times more abundant in the 30 μm filter), free-living (4 \times more abundant in 0.2 μm filter), and bacteria abundant in both fractions from density $\sigma_0 = 15.8$. The outer ring indicates the relative abundance of each OTU. Taxonomic groups with < 30 tags were not included in (c) for simplicity, but can be found in Tables S1–S8.

techniques (Fig. 6) but similarity indices are also similar. The Bray–Curtis similarity between $\sigma_0 = 15.3$ and 15.8 is 52% for TRFLP and 50% for V6 tags with > 1% relative abundance. The Bray–Curtis similarity between $\sigma_0 = 15.8$ and 16.1 is 40% and 43%, respectively.

Our V6 pyrosequence dataset corresponds well with previously published quantitative analyses. For these comparisons, it is important to note that cell counts from the suboxic zone at this station ($5 \pm 1\text{E}5$ cells mL^{-1} ; Table S1) were similar to values obtained on other cruises (Lin *et al.*, 2006), and that cell counts did not change appreciably throughout the suboxic zone (Table S1). Furthermore, the percentage of total V6 tag pyrosequences at each density surface was similar to previously reported values determined using more quantitative methods. For example, the proportion of V6 tag sequences at $\sigma_0 = 16.1$

assigned to the family Methylococcales (1%) is identical to the proportion of bacteria identified as Methylococcales (1%) in 2001 using quantitative PCR of 16S rRNA gene (Schubert *et al.*, 2006). The proportion of cells with bacterial chlorophyll *e* (0.5–1%) in 2001 (Manske *et al.*, 2005) is similar to the proportion of V6 tag sequences assigned to Chlorobi (0.6%). The proportions of *Candidatus* Scalindua sorokinii in 2001 (0.8%; Kuypers *et al.*, 2003) and sulfate reducers in 2003 (8%; Lin *et al.*, 2006) identified using FISH also matched closely with the proportion of V6 tag sequences assigned to these groups (0.8% and 11%, respectively). However, a few discrepancies should be noted. *Epsilonproteobacteria* were 1.4% of V6 tags at $\sigma_0 = 16.1$ in 2005, but 6% of DAPI stained cells were found to be *Epsilonproteobacteria* by FISH at the same station in 2003 (Lin *et al.*, 2006).

Gammaproteobacteria comprise 25% of V6 tag sequences, but only 6% were found using FISH (Lin *et al.*, 2006). As the *Gammaproteobacteria* are a phylogenetically diverse group, that discrepancy may be due to FISH probe mismatches to some sub-groups. Most surprisingly, *Bacteroidetes* comprised only 0.4% of V6 tag sequences, but 5% of cells were identified as *Bacteroidetes* in 2003 using FISH (Lin *et al.*, 2006). It is puzzling that TRFLP frag-

ments corresponding to *Bacteroidetes* sequences BS040 and BS035 (both appear as a 91-bp fragment using the MspI enzyme in Fig. S3) were identified in $\sigma_0 = 15.8$, but no corresponding V6 tags were found. No mismatch was found between these sequences and the V6 primer set. In summary, there is general agreement between the proportion of V6 pyrosequences and published quantitative analyses.

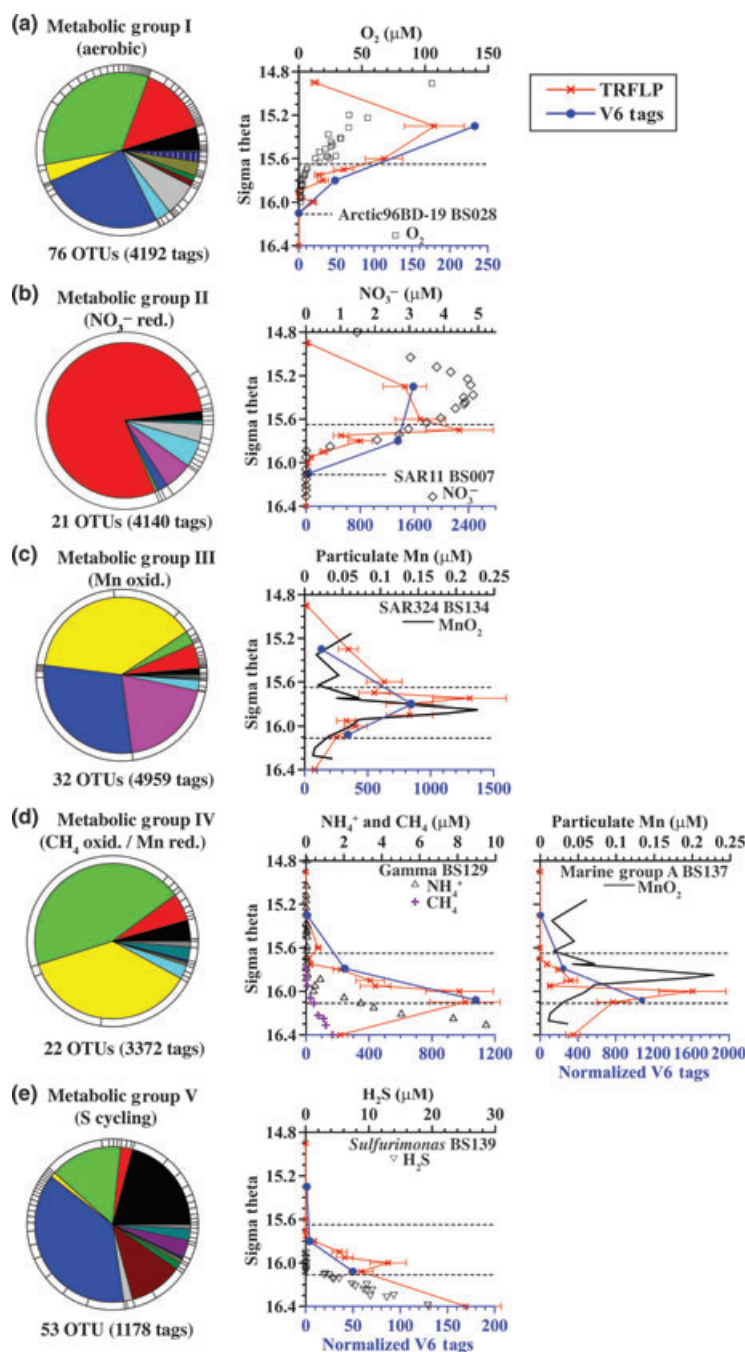


Fig. 6. Depth profiles of bacteria in the Black Sea and their taxonomy. Five bacterial depth profiles were predicted from chemical profiles and fluxes (Table 1). Pie charts indicate the taxonomy of all the V6 tag sequences placed in each category, using the color key from Fig. 2. More specific taxonomies can be found in the Tables S1–S8. Outer ring indicates the number of OTUs in each group, and the size of each section in the outer ring indicates the number of tags in each OTU. An example full-length sequence identified in both TRFLP chromatograms (in red) and V6 tag sequences (in blue) illustrates each depth profile. Relative fluorescent units for TRFLP peak heights are adjusted to match the scale for V6 tags. Profile types are as follows: (a) aerophilic, (b) nitrate reducing, (c) manganese oxidizing, (d) methane oxidizing, ammonia oxidizing, or manganese reducing, and (e) sulfur utilizing.

Discussion

The Black Sea is a permanently stratified basin. Chemical profiles occur in a predictable sequence on density surfaces through the Black Sea (Murray *et al.*, 1995), although decadal (Konovalov & Murray, 2001), interannual (Fuchsman *et al.*, 2008), and seasonal variability (Yakushev *et al.*, 2006) in the concentrations of chemical species have been observed in some instances. The Black Sea has been stratified for over 7000 years (Jones & Gagnon, 1994), which is in contrast with transiently oxygenated basins such as the Baltic Sea (Hannig *et al.*, 2007) or fjords such as Saanich Inlet (Manning *et al.*, 2010), where periodic oxygenation events affect microbial activity. Thus, one expects less temporal variability in the microbial community of the Black Sea than seen in these transiently oxygenated basins, but this has never been examined. We can compare our data to TRFLP data (with restriction enzyme MnlI) from three suboxic water samples collected during a Black Sea expedition in 1988 (Vetriani *et al.*, 2003). We have much greater confidence in our peak identifications, because we used multiple restriction enzymes (Engebretson & Moyer, 2003) and obtained TRFLP chromatograms of the clones themselves. We have, however, compared all TRFLP fragment sizes listed by Vetriani *et al.* with our TRFLP profiles. Of the TRFLP peaks listed by Vetriani *et al.* as being from the oxic zone, 45% were shared by our $\sigma_\theta = 14.9$ sample from 2005. Of the peaks listed as being from the suboxic zone, 60% were shared by at least one suboxic zone sample from 2005. Therefore, the microbial community appears to show remarkable continuity from 1988 to 2005, but some differences are apparent, and more research is needed to more closely examine temporal variability in the Black Sea. In general, however, the stability of Black Sea's suboxic zone, when compared with transiently anoxic basins where mixing and flushing occur, simplifies the conceptual task of understanding why certain organisms may be present at specific depths.

By examining nine suboxic/hypoxic depths with TRFLP, we saw that although bacterial communities from the suboxic zone do form a coherent cluster, the suboxic zone separates into three distinct microbial communities: upper, lower, and deep suboxic zones (Fig. S2). This data support objections that typical use of the term 'suboxic' is too broad to define microbial communities and geochemical processes (Canfield & Thamdrup, 2009). However, the term suboxic is still useful to define a depth range in the water column of interest here. Each sample for V6 tag pyrosequencing in this study was obtained from a distinct geochemical regime (Table 1). At $\sigma_\theta = 15.3$, representing the upper suboxic zone, O_2 (39 μM) and NO_3^- (4.8 μM) were high (Fig. 6a and b), and the concentration of particulate organic carbon was

relatively high (6 μM ; Fig. 1). At $\sigma_\theta = 15.8$, representing the lower suboxic zone, O_2 (1.8 μM) and NO_3^- (2.1 μM) decreased in concentration, and CH_4 and NH_4^+ were also detectable (Table 1). The concentrations of particulate manganese oxides were at their maximum at $\sigma_\theta = 15.8$ (Fig. 6c), and so we consider this depth to be part of the manganese oxidation zone. At $\sigma_\theta = 16.1$, representing the deep suboxic zone, both O_2 and NO_3^- were undetectable, but CH_4 (0.2 μM) and NH_4^+ (2 μM) were present along with a H_2S flux from sulfidic zone. The concentration of particulate manganese oxides at $\sigma_\theta = 16.1$ is less than at $\sigma_\theta = 15.8$ and continues to decrease with depth (Fig. 6c), and so we consider $\sigma_\theta = 16.1$ to be part of the manganese reduction zone. Thus, $\sigma_\theta = 15.3$, 15.8, and 16.1 represent three distinct geochemical regimes and three distinct bacterial communities (Figs S1 and S2; Table 1).

Predicting metabolisms

By examining the abundance of a bacterial taxon across large changes in geochemical gradients, one can make testable hypotheses about the metabolism of that taxon. We used normalized V6 tag abundance and normalized TRFLP peak height to represent bacterial abundance in this study. Our V6 tag abundances correspond well with previously reported values obtained with accepted quantitative techniques such as FISH and qPCR (see Results). Although the presence of DNA does not indicate metabolic activity, large differences in these DNA depth profiles that correspond to changes in the geochemical profiles probably reflect distinct zones of metabolic activity. This is particularly true for the Black Sea, which has maintained geochemical profiles at similar density surfaces at least since the 1960s (Konovalov & Murray, 2001) and probably much longer.

We used chemical fluxes (Table 1) to predict five general metabolic depth profiles (I–V) of organisms utilizing each oxidant or reductant: (I) oxygen utilization, (II) nitrate reduction, (III) manganese oxidation, (IV) oxidation of methane and ammonium or manganese reduction, and (V) sulfate reduction or sulfide oxidation. We then categorized each V6 OTU into one of these depth profiles (Metabolic Groups I–V). Known bacterial species falling into each of these depth profiles use metabolisms, consistent with the predictions ($n = 46$). In general, bacterial depth profiles measured by V6 tag sequences and by TRFLP peaks are equivalent (Fig. 6). Black Sea Groups I–V are quite different with respect to bacterial taxonomy (Fig. 6), and we discuss each of the five groups in detail below. Only four OTUs with significant abundances did not fit into any category (Table S6), including a *Nitrospina* relative, matching full-length sequence BS001, and a SUP05

Gammaproteobacteria matching phylotype BS077 (SUP05). These predictions are imperfect, and we acknowledge their hypothetical nature. The purpose here is to link uncultured sequence data to environmental information, and suggest testable hypotheses as to the metabolisms of these uncultured bacteria. As proof of concept, we also discuss below how this method appropriately categorized a few known and characterized organisms.

Metabolic Group I: microaerophilic bacteria

Oxygen concentrations and fluxes were highest at $\sigma_0 = 15.3$, an order of magnitude lower at $\sigma_0 = 15.8$, and undetectable at $\sigma_0 = 16.1$ (Fig. 6a). The first depth profile category, which is defined as high relative abundance at $\sigma_0 = 15.3$ (39 μM O_2) and then a steep decrease with depth, is consistent with microaerophily. Seventy-six OTUs (4192 tags) had this type of depth profile (Table S2). *Gammaproteobacteria* (including BS028 (Fig. 6a) from the Arctic96BD-19 cluster and BS024 of the SAR86 cluster), and *Deltaproteobacteria* (an unidentified SAR324 bacterium) dominated this depth profile with significant contributions from *Alphaproteobacteria* and *Verrucomicrobia* (Fig. 6a). Both aerobic heterotrophs (e.g. phylotype BS006 in the HTCC2207 cluster of oligotrophic aerobic heterotrophic isolates; Cho & Giovannoni, 2004) and aerobic autotrophs (e.g. phylotype BS003 a relative of ammonium oxidizer genus *Nitrosospira*; Teske *et al.*, 1994) shared this depth profile.

Metabolic Group II: NO_3^- reducing bacteria

High relative abundances at $\sigma_0 = 15.3$ (4.8 μM NO_3^-) and $\sigma_0 = 15.8$ (2.1 μM NO_3^-) and very low abundances at $\sigma_0 = 16.1$ (0 μM NO_3^- and no calculated NO_3^- flux) are consistent with nitrate utilization (Fig. 6b). This is a reasonable assumption even though some nitrate reduction may be inhibited by 39 μM O_2 (Oh & Silverstein, 1999) as found at $\sigma_0 = 15.3$. Nitrate reduction has been measured at higher oxygen concentrations in the laboratory, presumably in anoxic micro-environments (Korner & Zumft, 1989; Oh & Silverstein, 1999). Indeed, there was a high concentration of particulate organic carbon at $\sigma_0 = 15.3$ (Fig. 1), which promotes low oxygen niches. Twenty-one OTUs (4140 tags) have this type of depth profile (Table S2). Bacteria with this depth profile are dominated by *Alphaproteobacteria*, including an abundant SAR11 relative BS007 (Fig. 6b), with large contributions from *Actinobacteria* (BS079), *Verrucomicrobia*, and *Planctomycetes* (BS126). The categorization of BS079 and BS126 as nitrate reducers is at least consistent with knowledge about their most closely related cultivated isolates (Rossetti *et al.*, 2005; Fukunaga *et al.*, 2009).

Metabolic Group III: Mn oxidizers

A maximum in bacterial abundance at $\sigma_0 = 15.8$ is consistent with manganese oxidation, because $\sigma_0 = 15.8$ is the only depth sequenced for V6 tags inside the manganese oxidation zone (defined by the positive slope of particulate manganese oxides with depth; Fig. 6c). One could also imagine some nitrate reducing organisms that are sensitive to 39 μM oxygen having this depth profile. Thirty-two OTUs (4959 tags) have this profile (Table S3). Marine Group A (phlotypes BS100 and BS110), *Actinobacteria* (phylotype BS158), and *Deltaproteobacteria* (SAR324 phylotype BS134; Fig. 6c) are among the most common taxa with this profile.

Metabolic Group IV: CH_4 oxidizers and MnO_2 reducers

As there were upward methane fluxes at $\sigma_0 = 15.8$ and $\sigma_0 = 16.1$, V6 tag sequences of methane-oxidizing bacteria should be present at both depths. Ammonium fluxes mirrored methane fluxes (Table 1); however, organic matter respiration also produces ammonium throughout the water column. Manganese oxide reducers could also share this profile; $\sigma_0 = 16.1$ is in the manganese oxide reduction zone (defined by a negative slope of particulate manganese oxides with depth; Fig. 6d) while some manganese reduction is also expected to occur at $\sigma_0 = 15.8$. Methane oxidation and manganese reduction have even been linked in marine sediments (Beal *et al.*, 2009), although whether or not they are linked in the Black Sea remains unclear. Twenty-two OTUs (3372 tags) have a Group IV depth profile (Table S4), and *Gammaproteobacteria* (including phylotype BS129; Fig. 6d) and Marine Group A (including phylotype BS137; Fig. 6d) were the most common taxonomic groups. Sequences affiliated with Methylococcales (type I methane oxidizers; Bowman *et al.*, 1993) were found in this category, as were anammox bacteria related to *Cand. Scalindua sorokinii*. Although their V6 tag depth profiles are similar, from TRFLP, it seems likely that BS129 and BS137 (Fig. 6d) use different metabolisms. While *Gammaproteobacterium* BS129 smoothly increases with depth, Marine Group A BS137 has a sharp TRFLP peak maximum at $\sigma_0 = 16.0$. *Gammaproteobacterium* BS129 is closely related to sequence II8-19 (GU108534; Fig. 3), which was enriched in ^{13}C during a SIP experiment with bicarbonate (Glaubitze *et al.*, 2010). It might be expected that a methane-oxidizer would obtain its carbon from methane rather than bicarbonate. Ammonia-oxidizers, however, are autotrophic, and a *Gammaproteobacterium* mRNA sequence of the ammonium-oxidizing gene *amoA* was dominant in the lower suboxic zone in August 2005 (Lam *et al.*, 2007). Marine

Group A BS137 seems more likely to be a manganese-reducer, because its TRFLP peak height is highest at depths when net manganese oxide consumption is occurring (Fig. 6d).

Metabolic Group V: sulfur cycling bacteria

It is likely that the upward flux of sulfide affects the microbial community at $\sigma_0 = 16.1$ (Table 1). Sulfide was not measurable at this depth, but the detection limit for the method used was 3 μM (Konovalov *et al.*, 2003). As oxygen and nitrate are absent at this depth and MnO_2 and nitrite concentrations (0.04 μM) are low, fermentation and sulfate reduction may occur. Fifty-three OTUs (1178 tags) have this profile (Table S5), and the most dominant taxa are *Deltaproteobacteria* and *Gammaproteobacteria* (e.g. BS136), with important contributions from *Lentisphaera* and *Epsilonproteobacteria*. The *Deltaproteobacteria* are mostly represented by the group Desulfobacteraceae, which are associated with sulfate reduction (Finster *et al.*, 1997) and fermentation (Kendall *et al.*, 2006). Epsilonproteobacterial pyrosequences matched full-length sequence BS139 (Fig. 6e) of the *Sulfurimonas* genus (Fig. 3), a genus in which all the cultured isolates mediate sulfur oxidation (Inagaki *et al.*, 2003; Takai *et al.*, 2006).

In summary, although we cannot attribute a metabolism to an uncultured sequence, we can make useful, testable hypotheses by examining the depth profiles of individual phylotypes across a chemical gradient. These hypotheses should focus future investigations into the physiology of specific organisms in the Black Sea.

Aggregate-attached bacteria

Both bulk water and 30 μm pore size filter samples were obtained from the center of the suboxic zone ($\sigma_0 = 15.8$). Aggregates larger than 53 μm dominate the vertical mass flux in the ocean (Clegg & Whitfield, 1990; Amiel *et al.*, 2002). Therefore, bacteria caught on the 30 μm filter are likely to be mainly attached to sinking aggregates with some attached to large suspended particles. S-POC decreased from 14 μM in the oxic zone to 4 μM in the suboxic zone (Fig. 1) and C/N ratios were around 9 (C. Fuchsman, unpublished data), indicating that the particulate organic matter was at least partially degraded. The particulate sample is from a depth ($\sigma_0 = 15.8$) above the zone of chemosynthesis (Yilmaz *et al.*, 2006), and so this organic material probably sank from the euphotic zone. The presence of V6 tags related to diatom chloroplasts in the 30 μm fraction (Fig. 2) is consistent with a source from the euphotic zone. Particulate manganese oxides were also present at this depth (Table 1).

These data are one of the first instances of aggregate-associated bacteria being examined under suboxic conditions. Although the Black Sea suboxic zone is only 30–40 m wide, there should still be time for the low oxygen conditions to affect the aggregates. In 1988, the average settling speed of aggregates (0.5–5.5 mm diameter) in the suboxic zone was 11.7 m day^{-1} (Diercks & Asper, 1997). So, an average particle at $\sigma_0 = 15.8$ would have been under truly suboxic conditions for 10 m, or almost 1 day. A day is long enough to allow shifts in microbial communities (McCarren *et al.*, 2010).

The taxonomic classification of aggregate-associated bacteria in the Black Sea suboxic zone was significantly different from aggregate-associated bacteria in oxic environments. In the oxic Santa Barbara Channel, *Bacteroidetes*, *Planctomycetes*, and *Gammaproteobacteria* dominated in sinking aggregates (DeLong *et al.*, 1993), and in the highly oxygenated Arctic ocean, *Gammaproteobacteria* of the uncultured Arctic96B-1 and OM60 groups dominated aggregate-associated (> 60 μm) clone libraries (Kellogg & Deming, 2009). In the Black Sea suboxic zone, Marine Group A, *Deltaproteobacteria*, and *Planctomycetes* dominated the aggregate-associated fraction (> 30 μm) (Fig. 2). Many other groups were enriched in the Black Sea aggregate-associated fraction, including *Lentisphaera*, WS3, and *Epsilonproteobacteria*. The aggregate-associated community in the Black Sea suboxic zone appears to be distinct from those found in oxic environments.

We consider the aggregate-associated community to be the bacteria on the 30 μm filter. However, some abundant free-living bacteria may have been trapped in the 30 μm filter. Therefore, we have distinguished between aggregate-associated bacteria and bacteria expected to be actually aggregate-attached according to their relative abundance in the bulk water sample compared with the 30 μm filter. We consider aggregate-attached bacteria to have 5 \times greater abundance in the particulate sample than in the bulk water sample, and consider free-living bacteria to have 4 \times greater abundance in the bulk water. In this case, even though SAR11 relatives were found on the 30 μm filter, they are considered free-living due to their extremely high abundance in the bulk water sample. Of the 125 OTUs with more than five V6 tag sequences found in the 30 μm sample, 53 OTUs are considered here to be aggregate-attached (Fig. 5c, column 1 and Table S7). Thirty-seven OTUs, with more than five V6 tag sequences found in the $\sigma_0 = 15.8$ water sample, had 4 \times greater abundance in the bulk water, and are considered here to be free-living (Fig. 5c, column 2), whereas 36 OTUs were abundant in both the aggregate and bulk water samples at $\sigma_0 = 15.8$ (Fig. 5c, column 3). Free-living and aggregate-attached OTUs have strikingly different community structures (Fig. 5c). *Alphaproteobacteria* in

the SAR11 clade dominated the free-living fraction. *Planctomycetes*, *Deltaproteobacteria*, Marine Group A, *Lentisphaera*, *Epsilonproteobacteria*, WS3, and *Deinococci* were enriched in the aggregate-attached fraction. A large number of OTUs (111) were shared only between the aggregate-attached fraction at $\sigma_\theta = 15.8$ and bulk water at $\sigma_\theta = 16.1$, a depth influenced by sulfide (Fig. 5b). These OTUs are shared in spite of the fact that the sinking aggregates would not yet have had contact with that depth. These OTUs include members of the *Epsilonproteobacteria*, WS3, *Lentisphaera*, and *Deinococci*. Some OTUs found in the aggregate-attached fraction were not significant in the bulk water at any depth. These include some members of the *Planctomycetes* (BS097, BS109) and the *Deltaproteobacteria*.

The overlap of many OTUs between the particulate sample at $\sigma_\theta = 15.8$ and the bulk water sample at $\sigma_\theta = 16.1$, a sample that was influenced by the sulfide flux from the anoxic zone (Table 1), suggests that S cycling may be occurring in the aggregate. This is supported by the presence of aggregate-attached *Epsilonproteobacteria* from the *Sulfurimonas* genus (BS139) closely related to *S. denitrificans* and *S. autotrophica* (Fig. 3). All cultured members of this genus have been found to oxidize sulfide with NO_3^- or O_2 (Inagaki *et al.*, 2003; Takai *et al.*, 2006). Clone BS077, a SUP05 which is aggregate-associated and also abundant in the bulk water sample, is closely related to SUP05 from Saanich Inlet (Fig. 3), which is implicated in sulfur oxidation by metagenomic sequences (Walsh *et al.*, 2009). Sulfur oxidation genes from SUP05 were also present and expressed in an oceanic oxygen minimum zone (Canfield *et al.*, 2010; Stewart *et al.*, 2011). Many aggregate-attached V6 tags were also assigned to Desulfobulbaceae and Desulfuromonadales, two potentially sulfate reducing orders of bacteria. Thus, we have candidates for both sulfate reduction and sulfide oxidation potentially attached to particles. In addition, aggregate-attached Marine Group A bacterium BS137 is associated with manganese reduction (Fig. 6e). Aggregate-associated bacteria also include Marine Group A bacteria, which are linked to manganese oxidation (e.g. BS110), and *Actinobacteria* (e.g. BS079) associated with nitrate reduction (Fig. 6; Tables S3 and S4). Therefore, we predict that the aggregates hosted a variety of metabolisms.

It is unclear whether sulfate reduction is feasible at $\sigma_\theta = 15.8$, because sulfate reduction is typically inhibited by oxygen. Sulfate reduction has been measured in the Oxygen Minimum Zone off of Chile (Canfield *et al.*, 2010) even though sulfide concentrations were below detection. Oxygen concentrations in the OMZ, however, were significantly lower than those measured at $\sigma_\theta = 15.8$ in the Black Sea (20 nM vs. 2 μM). In the following, we evaluate the possibility of sulfur reduction inside aggregates from the suboxic zone with a simple model of oxy-

gen penetration into the aggregate. Nutrient gradients in and around aggregates can be described using molecular diffusion across a diffusive boundary layer that surrounds the aggregates (Alldredge & Cohen, 1987; Ploug *et al.*, 1997). Oxygen utilization in particles is not transport-limited in fully oxygenated seawater, but rather reaction-limited, which is why aggregates are generally not anoxic (Ploug, 2001). However, calculations predict that at *c.* 25 μM ambient O_2 , oxygen utilization becomes transport limited (Ploug, 2001). Both oxygen (2 μM) and nitrate (2 μM) should be transport limited at $\sigma_\theta = 15.8$. The volumetric oxygen respiration rate for a 1 mm diameter particle with a 0.17 mm boundary layer thickness (after Ploug *et al.*, 1997) is 162 $\mu\text{mol cm}^{-3} \text{ day}^{-1}$ organic carbon in the aggregate at $\sigma_\theta = 15.3$, but much lower (4 $\mu\text{mol cm}^{-3} \text{ day}^{-1}$) in the aggregate at $\sigma_\theta = 15.8$. It seems reasonable to expect that oxygen would not reach the center of such an aggregate at $\sigma_\theta = 15.8$.

We suggest that an aggregate under suboxic conditions contains multiple niches. An outer layer would contain organisms that utilize nitrate or oxygen, whereas in the center of the aggregate, sulfate reduction and manganese reduction might occur. Sulfate reduction produces sulfide (and ammonium) that would be oxidized in the outer layer of the particle. This layering of aerobic and anaerobic bacteria in aggregates under suboxic conditions has been seen in wastewater treatment plants (Vlaeminck *et al.*, 2010). Thus, we expect a large diversity of metabolisms to occur in a relatively small volume. This diversity of metabolisms under low oxygen conditions may be why the V6 region of 16S rRNA gene aggregate-associated community was the most diverse in this study (Fig. 5a). Our results contrast to the highly oxygenated Arctic Ocean, where the aggregate-associated bacterial community was less diverse than the free-living community (Kellogg & Deming, 2009). This difference is consistent with the fact that in oxygen-saturated water, aggregates can only undergo transitory anoxic conditions and that sustained sulfate reduction and methanogenesis cannot occur (Ploug *et al.*, 1997).

Conclusions

The combination of in-depth sequencing of the V6 region of 16S rRNA gene to provide information about the entire microbial community, TRFLP to give spatial resolution, full-length clones to give these techniques taxonomic resolution, and extensive chemical profiles to provide ecological context have allowed us to examine bacterial communities of the suboxic and hypoxic zones of the Black Sea more comprehensively than ever before.

Five general depth profiles of bacterial abundance were identified and correlated with geochemical data, and the metabolisms that might correspond to each of these

depth profiles were predicted. These predictions, although imperfect, provide testable hypotheses regarding the metabolic strategies of uncultured bacteria in the Black Sea suboxic zone. A series of metagenomic analyses of the Black Sea suboxic zone would better link bacterial identity to metabolic genes. Future work could include experiments (e.g. stable isotope probing) designed to explicitly test for predicted metabolic reactions.

Our study also highlights the effect of low redox conditions on the microbial diversity of sinking aggregates. Free-living and aggregate-attached OTUs had strikingly different taxonomies. Aggregate-attached OTUs included bacteria linked to sulfate reduction and sulfide oxidation, implying more reducing E_h conditions in aggregate interiors than found in the ambient water.

Acknowledgements

We thank Ekaterina Andreishcheva and ICoMM for running the V6 samples; Sue Huse for providing GAST taxonomies; Patrick Schloss for use of his programs; and P. Swift, J. Gilbert, and D. Field for use of DaisyChopper. We thank Brad Tebo for providing particulate manganese data. Thanks also to Brian Oakley for help in collecting the DNA samples, Barbara Paul and Evgeniy Yakushev for running nutrient samples, and Sergey Kononov and Alexander Romanov for providing oxygen and sulfide data. We also thank G. Rocard and the reviewers for comments on the manuscript. C.A.F., J.B.K., and W.J.B. were supported by IGERT traineeships in Astrobiology under NSF grant 05-04219. This work was also supported by NSF OISE 0637866, OISE 0637845, and OCE 0649223.

References

- Allredge AL & Cohen Y (1987) Can microscale chemical patches persist in the sea? Microelectrode study of marine snow, fecal pellets. *Science* **235**: 689–691.
- Amiel D, Cochran JK & Hirschberg DJ (2002) $^{234}\text{Th}/^{238}\text{U}$ disequilibrium as an indicator of the seasonal export flux of particulate organic carbon in the North Water. *Deep Sea Res II* **49**: 5191–5209.
- Armstrong FA, Stearns CR & Strickland JDH (1967) The measurement of upwelling and subsequent biological processes by means of the Technicon AutoAnalyzer and associated equipment. *Deep Sea Res* **14**: 381–389.
- Beal EJ, House CH & Orphan VJ (2009) Manganese- and iron-dependent marine methane oxidation. *Science* **325**: 184–187.
- Bowman JP, Sly LI, Nichols PD & Hayward AC (1993) Revised taxonomy of the methanotrophs: description of *Methylobacter* gen. nov., emendation of *Methylococcus*, validation of *Methylosinus* and *Methylocystis* species, and a proposal that the family Methylococcaceae includes only the group I methanotrophs. *Int J Syst Bacteriol* **43**: 735–753.
- Brazelton WJ, Ludwig KA, Sogin ML, Andreishcheva EN, Kelley DS, Shen C, Edwards RL & Baross JA (2010) Archaea and bacteria with surprising microdiversity show shifts in dominance over 1,000-year time scales in hydrothermal chimneys. *P Natl Acad Sci USA* **107**: 1612–1617.
- Brewer PG & Spencer DW (1971) Colorimetric determination of manganese in anoxic waters. *Limnol Oceanogr* **16**: 107–110.
- Buesseler KO, Livingston HD & Casso SA (1991) Mixing between oxic and anoxic waters of the Black Sea as traced by Chernobyl cesium isotopes. *Deep Sea Res* **38** (suppl. 2A): S725–S746.
- Campanella JJ, Bitincka L & Smalley J (2003) MatGAT: an application that generates similarity/identity matrices using protein or DNA sequences. *BMC Bioinform* **4**: 29.
- Canfield DE & Thamdrup B (2009) Towards a consistent classification scheme for geochemical environments, or, why we wish the term ‘suboxic’ would go away. *Geobiology* **7**: 385–392.
- Canfield DE, Stewart FJ, Thamdrup B, De Brabandere L, Dalsgaard T, Delong EF, Revsbech NP & Ulloa O (2010) A cryptic sulfur cycle in oxygen-minimum-zone waters off the Chilean coast. *Science* **330**: 1375–1378.
- Carlson CA, Morris R, Parsons R, Treusch AH, Giovannoni SJ & Vergin K (2009) Seasonal dynamics of SAR11 populations in the euphotic and mesopelagic zones of the northwestern Sargasso Sea. *ISME* **3**: 283–295.
- Caspers H (1957) Black Sea and Sea of Azov. *Treatise on Marine Ecology and Paleocology*, Vol. 67 (Hedgpeth JW, ed), pp. 801–890. Geological Society of America Memoirs, New York.
- Cho J & Giovannoni SJ (2004) Cultivation and growth characteristics of a diverse group of oligotrophic marine Gammaproteobacteria. *Appl Environ Microbiol* **70**: 432–440.
- Clegg SL & Whitfield M (1990) A generalized model for the scavenging of trace metals in the open ocean – I. Particle cycling. *Deep Sea Res* **37**: 809–832.
- Clement BG, Luther GW III & Tebo BM (2009) Rapid, oxygen-dependent microbial Mn(II) oxidation kinetics at sub-micromolar oxygen concentrations in the Black Sea suboxic zone. *Geochim Cosmochim Acta* **73**: 1878–1889.
- Cline JD (1969) Spectrophotometric determination of hydrogen sulfide in natural waters. *Limnol Oceanogr* **14**: 454–458.
- Codispoti LA, Friederich GE, Murray JW & Sakamoto CM (1991) Chemical variability in the Black Sea: implications of data obtained with continuous vertical profiling system that penetrated the oxic-anoxic interface. *Deep Sea Res* **38**: S691–S710.
- DeLong EF, Franks DG & Allredge AL (1993) Phylogenetic diversity of aggregate-attached vs. free-living marine bacterial assemblages. *Limnol Oceanogr* **38**: 924–934.
- DeSantis TZ, Hugenholtz P, Keller K, Brodie E, Larsen N, Piceno YM, Phan R & Andersen GL (2006) NAST: a

- multiple sequence alignment server for comparative analysis of 16S rRNA genes. *Nucleic Acids Res* **34**: W394–W399.
- Diercks AR & Asper VL (1997) In situ settling speeds of marine snow aggregates below the mixed layer: Black Sea and Gulf of Mexico. *Deep Sea Res I* **44**: 385.
- Engebretson JJ & Moyer CL (2003) Fidelity of select restriction endonucleases in determining microbial diversity of terminal-restriction fragment length polymorphism. *Appl Environ Microbiol* **69**: 4823–4829.
- Finster K, Liesack W & Tindall BJ (1997) *Desulfospira joergensenii*, gen. nov., sp. nov., a new sulfate-reducing bacterium isolated from marine surface sediment. *Syst Appl Microbiol* **20**: 201–208.
- Fuchsman CA, Konovalov SK & Murray JW (2008) Concentration and natural stable isotope profiles of nitrogen species in the Black Sea. *Mar Chem* **111**: 90–105.
- Fukunaga Y, Kurahashi M, Sakiyama Y, Ohuchi M, Yokota A & Harayama S (2009) *Phycisphaera mikurensis* gen. nov., sp. nov., isolated from a marine alga, and proposal of Phycisphaeraceae fam. Nov., Phycisphaerales ord. Nov. and Phycisphaerae classes nov. in the phylum Planctomycetes. *J Gen Appl Microbiol* **55**: 267–275.
- Glaubitz S, Labrenz M, Jost G & Jurgens K (2010) Diversity of active chemolithoautotrophic prokaryotes in the sulfidic zone of a Black Sea pelagic redoxcline as determined by rRNA-based stable isotope probing. *FEMS Microbiol Ecol* **74**: 32–41.
- Gregg MC & Yakushev E (2005) Surface ventilation of the Black Sea's cold intermediate layer in the middle of the western gyre. *Geophys Res Lett* **32**: L03604.
- Grote J, Jost G, Labrenz M, Herndl GJ & Jurgens K (2008) *Epsilonproteobacteria* represent the major portion of chemolithoautotrophic bacteria in sulfidic waters of pelagic redoxclines of the Baltic and Black Seas. *Appl Environ Microbiol* **74**: 7546–7551.
- Hannig M, Lavik G, Kuypers MMM, Woebken D, Martens-Habbena W & Jurgens K (2007) Shift from denitrification to anammox after inflow events in the central Baltic Sea. *Limnol Oceanogr* **52**: 1336–1345.
- Hewson I & Fuhrman JA (2006) Improved strategy for comparing microbial assemblage fingerprints. *Microb Ecol* **51**: 147–153.
- Huber JA, Welch DM, Morrison HG, Huse SM, Neal PR, Butterfield DA & Sogin ML (2007) Microbial population structures in the deep marine biosphere. *Science* **318**: 97–100.
- Huse SM, Huber JA, Morrison HG, Sogin ML & Welch DM (2007) Accuracy and quality of massively parallel DNA. *Genome Biol* **8**: R143.
- Huse SM, Dethlefsen L, Huber JA, Welch DM, Relman DA & Sogin ML (2008) Exploring microbial diversity and taxonomy using SSU rRNA hypervariable tag sequencing. *PLoS Genet* **4**: e1000255.
- Inagaki F, Takai K, Hideki KI, Neilson KH & Horikishi K (2003) *Sulfuromonas autotrophica* gen. nov., spp nov., a novel sulfur oxidizing epsilon-proteobacterium isolated from hydrothermal sediments in the mid-Okinawa Trough. *Int J Syst Evol Microbiol* **53**: 1801–1805.
- Ivanov LI & Samodurov AS (2001) The role of lateral fluxes in ventilation of the Black Sea. *J Mar Syst* **31**: 159–174.
- Jones GA & Gagnon AR (1994) Radiocarbon chronology of Black Sea sediments. *Deep-Sea Res I* **41**: 531–557.
- Jumas-Bilak E, Roudiere L & Marchandin H (2009) Description of 'Synergistetes' phyl. nov. and emended description of phylum 'Deferribacteres' and of the family Syntrophomonadaceae, phylum 'Firmicutes.' *Int J Syst Evol Microbiol* **59**: 1028–1035.
- Kellogg CTE & Deming JW (2009) Comparison of free-living, suspended particle, and aggregate-associated bacterial and archaeal communities in the Laptev Sea. *Aquat Microb Ecol* **57**: 1–18.
- Kendall MM, Liu Y & Boone DR (2006) Butyrate- and propionate-degrading syntrophs from permanently cold marine sediments in Skan Bay, Alaska, and description of *Algorimarina butyrica* gen. Nov., sp. nov. *FEMS Microbiol Lett* **262**: 107–114.
- Kessler JD, Reeburgh WS & Tyler SC (2006) Controls on methane concentration and stable isotope distributions in the water columns of the Black Sea and Cariaco Basin. *Global Biogeochem Cycles* **20**: GB4004.
- Kirkpatrick J, Oakley B, Fuchsman C, Srinivasan S, Staley JT & Murray JW (2006) Diversity and distribution of Planctomycetes and related bacteria in the suboxic zone of the Black Sea. *Appl Environ Microbiol* **72**: 3079–3083.
- Konovalov SK & Murray JW (2001) Variations in the chemistry of the Black Sea on a time scale of decades (1960–1995). *J Mar Syst* **31**: 217–243.
- Konovalov SK, Luther GW III, Friederich GE, et al. (2003) Lateral injection of oxygen with the Bosphorus plume-fingers of oxidizing potential in the Black Sea. *Limnol Oceanogr* **48**: 2369–2376.
- Korner H & Zumft WG (1989) Expression of denitrification enzymes in response to dissolved oxygen level and respiratory substrate in continuous culture of *Pseudomonas stutzeri*. *Appl Environ Microbiol* **55**: 1670–1676.
- Kuypers MMM, Sliekers AO, Lavik G, Schmid M, Jorgensen BB, Kuenen JG, Damste JSS, Strous M & Jetten MSM (2003) Anaerobic ammonium oxidation by anammox bacteria in the Black Sea. *Nature* **422**: 608–611.
- Lam P, Jensen MM, Lavik G, McGinnis DF, Muller B, Schubert CJ, Amann R, Thamdrup B & Kuypers MMM (2007) Linking crenarchaeal and bacterial nitrification to anammox in the Black Sea. *P Natl Acad Sci USA* **104**: 7104–7109.
- Lane DJ (1991) 16S/23S rRNA sequencing. *Nucleic Acid Techniques in Bacterial Systematics* (Stackebrand E & Goodfellow M, eds), pp. 115–175. Wiley, New York.
- Lewis BL & Landing WM (1991) The biogeochemistry of manganese and iron in the Black Sea. *Deep Sea Res* **38**: S773–S804.
- Lin X, Wakeham SG, Putnam IF, Astor YM, Scranton MI, Chistoserdov AY & Taylor GT (2006) Comparison of vertical distributions of prokaryotic assemblages in the

- Anoxic Cariaco basin and the Black Sea by use of fluorescence in situ hybridization. *Appl Environ Microbiol* **72**: 2679–2690.
- Manning CC, Hamme RC & Bourbonnais A (2010) Impact of deep-water renewal events on fixed nitrogen loss from seasonally-anoxic Saanich Inlet. *Mar Chem* **122**: 1–10.
- Manske AK, Glaeser J, Kuypers MMM & Overmann J (2005) Physiology and phylogeny of green sulfur bacteria forming a monospecific phototrophic assemblage at the depth of 100 meters in the Black Sea. *Appl Environ Microbiol* **71**: 8049–8060.
- McCarren J, Becker JW, Repeta DJ, Shi YM, Young CR, Malmstrom RR, Chisholm SW & De Long EF (2010) Microbial community transcriptomes reveal microbes and metabolic pathways associated with dissolved organic matter turnover in the sea. *P Natl Acad Sci USA* **107**: 16420–16427.
- Murray JW, Codispoti LA & Friederich GE (1995) Oxidation-reduction environments: the suboxic zone in the Black Sea. *Aquatic Chemistry: Interfacial and Interspecies Processes. Advances in Chemistry Series*, Vol. 224 (Huang CP, O'Melia CR & Morgan JJ, eds), pp. 157–176. American Chemical Society, Washington, DC.
- Muyzer G, De Waal EC & Uitterlinden AG (1993) Profiling of complex microbial populations by denaturing gradient gel electrophoresis analysis of polymerase chain reaction-amplified genes coding for 16S rRNA. *Appl Environ Microbiol* **59**: 695–700.
- Oakley BO, Francis CA, Roberts KJ, Fuchsman CA, Srinivasan S & Staley JT (2007) Analysis of nitrite reductase (*nirK* and *nirS*) genes and cultivation reveal depauperate community of denitrifying bacteria unique to the Black Sea suboxic zone. *Environ Microbiol* **9**: 118–130.
- Oh J & Silverstein J (1999) Oxygen inhibition of activated sludge denitrification. *Water Res* **33**: 1925–1937.
- Ploug H (2001) Small scale oxygen fluxes and remineralization in sinking aggregates. *Limnol Oceanogr* **46**: 1624–1631.
- Ploug H, Kuhl M, Buchholz-Cleven B & Jorgensen BB (1997) Anoxic aggregates – an ephemeral phenomenon in the pelagic environment? *Aquat Microb Ecol* **13**: 285–294.
- Polz MF & Cavanaugh CM (1998) Bias in template-to-product ratios in multitemplate PCR. *Appl Environ Microbiol* **64**: 3724–3730.
- Rainey FA, Ward N, Sly LI & Stackebrandt E (1994) Dependence on the taxon composition of clone libraries for PCR amplified, naturally occurring 16S rDNA, on the primer pair and the cloning system used. *Experientia* **50**: 796–797.
- Rossetti S, Tomei MC, Nielsen PH & Tandoi V (2005) “*Microthrix parvicella*”, a filamentous bacterium causing bulking and foaming in activated sludge systems: a review of current knowledge. *FEMS Microbiol Rev* **29**: 49–64.
- Schloss PD & Handelsman J (2005) Introducing DOTUR, a computer program for defining operational taxonomic units and estimating species richness. *Appl Environ Microbiol* **71**: 1501–1506.
- Schloss PD & Handelsman J (2006) Introducing SONS, a tool for operational taxonomic unit-based comparisons of microbial community memberships and structures. *Appl Environ Microbiol* **72**: 6773–6779.
- Schubert CJ, Coolen MJL, Neretin LN, Schippers A, Abbas B & Durisch-Kaiser E *et al.* (2006) Aerobic and anaerobic methanotrophs in the Black Sea water column. *Environ Microbiol* **8**: 1844–1856.
- Simon M, Grossart H, Schweitzer B & Ploug H (2002) Microbial ecology of organic aggregates in aquatic ecosystems. *Aquat Microb Ecol* **28**: 175–211.
- Slawky G & MacIsaac JJ (1972) Comparison of two automated ammonium methods in a region of coastal upwelling. *Deep Sea Res* **19**: 521–524.
- Sogin ML, Morrison HG, Huber JA, Welch DM, Huse SM, Neal PR, Arrieta JM & Herndl GJ (2006) Microbial diversity in the deep sea and the underexplored “rare biosphere.” *P Natl Acad Sci USA* **103**: 12115–12120.
- Sorokin YI (1983) The Black Sea. *Ecosystems of the World 26: Estuaries and Enclosed Seas* (Ketchum BH, ed), pp. 253–292. Elsevier, Amsterdam.
- Stewart FJ, Ulloa O & DeLong EF (2011) Microbial metatranscriptomics in a permanent marine oxygen minimum zone. *Environ Microbiol*. DOI: 10.1111/j.1462-2920.2010.02400.x.
- Takai K, Suzuki M, Nakagawa S, Miyazaki M, Suzuki Y, Inagaki F & Horikoshi K (2006) *Sulfurimonas parvalvinellae* sp nov., a novel mesophilic, hydrogen- and sulfur – oxidizing chemolithoautotroph within the *Epsilonproteobacteria* isolated from a deep-sea hydrothermal vent polychaete nest, reclassification of *Thiomicrospira denitrificans* as *Sulfurimonas denitrificans* comb. nov and emended description of the genus *Sulfurimonas*. *Int J Syst Evol Microbiol* **56**: 1725–1733.
- Teske A, Alm E, Regan JM, Toze S, Rittmann BE & Stahl DA (1994) Evolutionary relationships among ammonia-oxidizing and nitrite-oxidizing bacteria. *J Bacteriol* **176**: 6623–6630.
- Tolmazin D (1985) Changing coastal oceanography of the Black Sea. I: northwest shelf. *Prog Oceanogr* **15**: 217–276.
- Vlaeminck SE, Terada A, Smets BF *et al.* (2010) Aggregate size and architecture determine microbial activity balance for one-stage partial nitrification and anammox. *Appl Environ Microbiol* **76**: 900–909.
- Vetriani C, Tran HV & Kerkhof LJ (2003) Fingerprinting microbial assemblages from the oxic/anoxic chemocline of the Black Sea. *Appl Environ Microbiol* **69**: 6481–6488.
- Vinogradov MY & Nalbandov YR (1990) Effect of changes in water density on the profiles of physicochemical and biological characteristics in the pelagic ecosystem of the Black Sea. *Oceanol* **30**: 567–573.
- Walsh DA, Zaikova E, Howes CG, Song YC, Wright JJ, Tringe SG, Tortell PD & Hallam SJ (2009) Metagenome of a versatile chemolithoautotroph from expanding oceanic dead zones. *Science* **326**: 578–582.

- Wobken D, Lam P, Kuypers MMM, Naqvi SWA, Kartal B, Strous M, Jetten MSM, Fuchs BM & Amann R (2008) A microdiversity study of anammox bacteria reveals a novel *Candidatus Scalindua* phylotype in marine oxygen minimum zones. *Environ Microbiol* **10**: 3106–3119.
- Yakushev EV, Chasovnikov VK, Debolskaya EI, Egorov AV, Makkaveev PN, Pakhomova SV, Podymov OI & Yakubenko VG (2006) The northeastern Black Sea redox zone: hydrochemical structure and its temporal variability. *Deep Sea Res II* **53**: 1769–1786.
- Yılmaz A, Çoban-Yıldız Y, Morkoç E & Bologa A (2006) Surface and mid-water sources of organic carbon by phyto- and chemo-autotrophic production in the Black Sea. *Deep-Sea Res II* **53**: 1988–2004.

Supporting Information

Additional Supporting Information may be found in the online version of this article:

Fig. S1. Depth profiles, using a density scale, for oxygen (squares), sulfide (triangles), nitrate (circles), nitrite (diamonds), ammonium (x), methane (crosses), and particulate manganese (bold squares) from the Western Central Gyre of the Black Sea in March 2005.

Fig. S2. Cluster of community similarities calculated from TRFLP profiles from depths throughout the oxygenated, suboxic, and sulfidic layers.

Fig. S3. TRFLP chromatograms from the suboxic zone, obtained using the enzyme MspI.

Fig. S4. TRFLP chromatograms from the deep suboxic and sulfidic zones, obtained using the enzyme MspI.

Table S1. Cell counts from the suboxic zone.

Table S2. Depth Profile Metabolic Group I: The number of normalized tags at each depth for each unique OTU in this depth profile as well as their lifestyle and taxonomy.

Table S3. Depth Profile Metabolic Group II: The number of normalized tags at each depth for each unique OTU in this depth profile as well as their lifestyle and taxonomy.

Table S4. Depth Profile Metabolic Group III: The number of normalized tags at each depth for each unique OTU in this depth profile as well as their lifestyle and taxonomy.

Table S5. Depth Profile Metabolic Group IV: The number of normalized tags at each depth for each unique OTU in this depth profile as well as their lifestyle and taxonomy.

Table S6. Depth Profile Metabolic Group V: The number of normalized tags at each depth for each unique OTU in this depth profile as well as their lifestyle and taxonomy.

Table S7. Unassigned Depth Profile: The number of normalized tags at each depth for each unique OTU in this depth profile as well as their lifestyle and taxonomy.

Table S8. Aggregate-attached bacteria: The number of normalized tags at each depth for each unique OTU as well as their taxonomy.

Please note: Wiley-Blackwell is not responsible for the content or functionality of any supporting materials supplied by the authors. Any queries (other than missing material) should be directed to the corresponding author for the article.